Aerosol Science and Technology

ISSN: 0278-6826 (Print) 1521-7388 (Online) Journal homepage: http://www.tandfonline.com/loi/uast20

Characterization of Wintertime Reactive Oxygen Species Concentrations in Flushing, New York

Prasanna Venkatachari , Philip K. Hopke , William H. Brune , Xinrong Ren , Robert Lesher , Jingqui Mao & Michael Mitchell

To cite this article: Prasanna Venkatachari , Philip K. Hopke , William H. Brune , Xinrong Ren , Robert Lesher , Jingqui Mao & Michael Mitchell (2007) Characterization of Wintertime Reactive Oxygen Species Concentrations in Flushing, New York, Aerosol Science and Technology, 41:2, 97-111, DOI: 10.1080/02786820601116004

To link to this article: http://dx.doi.org/10.1080/02786820601116004

Published online: 17 Jan 2007.

Submit your article to this journal

Article views: 317

View related articles

Citing articles: 36 View citing articles

Full Terms & Conditions of access and use can be found at
http://www.tandfonline.com/action/journalInformation?journalCode=uast20

Download by: [University of North Texas] **Date:** 06 January 2017, At: 02:59

Aerosol Science and Technology, 41:97–111, 2007
Copyright © American Association for Aerosol Research
ISSN: 0278-6826 print / 1521-7388 online
DOI: 10.1080/02786820601116004

Characterization of Wintertime Reactive Oxygen Species Concentrations in Flushing, New York

Prasanna Venkatachari,[1] Philip K. Hopke,[1] William H. Brune,[2] Xinrong Ren,[2] Robert Lesher,[2] Jingqui Mao,[2] and Michael Mitchell[2]
[1]*Department of Chemical Engineering, Clarkson University, Potsdam, New York, USA*
[2]*Department of Meteorology, Penn State University, University Park, Pennsylvania, USA*

One of the main hypotheses for the species causing the observed health effects of ambient particulate matter is peroxides and other reactive oxygen species (ROS). However, there is currently very little data available on the concentrations of particle-bound ROS or their behavior in different physical locations and seasons. The concentrations of particle-bound ROS were determined for various size fractions of the aerosol, ranging from 10 nm to 18 μm, in Flushing, New York during the period of January and early February 2004. Sampling was carried out at 3-hour intervals using a MOUDI^{TM} cascade impactor. The collected particles were treated with the non-fluorescent probe dichlorofluorescin (DCFH) that fluoresces when oxidized by the presence of ROS. The measured fluorescent intensities were converted into equivalent hydrogen peroxide concentrations, which were used as indicators of ROS reactivity, by calibrations using H_2O_2 standards. Diurnal profiles of the ROS concentrations were obtained. Correlations of the particulate ROS concentrations with the intensity of photochemical reaction, estimated secondary organic carbon (SOC) and gas phase OH and HO_2 radical concentrations were explored. The intensity of photochemical reactions and gas phase radical concentrations were found to be moderate factors affecting particulate ROS concentrations. The concentrations of ROS were found to be higher in the submicron size particles of the ambient aerosol.

INTRODUCTION

Epidemiological studies have reported a positive correlation between particulate matter (PM) concentrations and human morbidity and mortality (Dockery et al. 1992). These associations persist after adjustment for potential confounders and are thought to be causal. PM is composed of solid and liquid particles that are emitted by sources such as motor vehicles, roads, smokestacks, forest fires, windblown soil, volcanic emissions, sea spray, and so on. Although there have been significant advances in our understanding of the dynamics of the atmospheric aerosol, the mechanisms underlying the aforementioned responses have not yet been established. There have been continuing efforts to identify biologically active chemical species that may cause a disproportionate fraction of the adverse health effects. Of particular importance to particle toxicology are combustion particles that have a core of elemental carbon coated with a layer of organic hydrocarbons, metals, nitrates, and sulfates, all of which may play a role in particle toxicity. It has been suggested that particle toxicity arises through oxidative challenges to the lung, through the metal-catalyzed formation of reactive oxygen species (ROS) via Fenton-type reactions (Stohs and Bagchi 1995) at the target sites, at concentrations that overwhelm endogenous antioxidant systems, causing inflammation and leading to systemic dysfunctions. It needs to be recognized that there are ROS present in the atmosphere associated with respirable particles to which we are exposed. Mauderly (1998) has also proposed peroxides as one of the chemical species that might be associated with the adverse health effects observed for fine particles. The presence of particle-bound ROS that could be formed from a variety of anthropogenic and biogenic reactive hydrocarbon species could help to explain the uniformity of particle effects across a wide variety of locations in spite of large differences in the chemical composition of the particulate matter.

The chemical composition of the atmosphere is largely controlled by the presence of various oxidants in the atmosphere that effectively determine the lifetime of many natural and anthropogenic pollutants such as methane (CH_4), carbon monoxide (CO), non-methane hydrocarbons, nitrogen oxides (NO_x), and sulfur dioxide (SO_2). In turn, these pollutants can affect the level of oxidants and thus, affect the atmosphere's response to future perturbations. Oxygen-containing free radicals such as the hydroxyl (OH), hydroperoxyl (HO_2) and organic peroxyl radicals (RO_2), molecules like H_2O_2 and organic peroxides and ions

Received 24 January 2006; accepted 13 November 2006.
This work was supported by EPA Science to Achieve Results Program through a subcontract from the University of Rochester PM and Health Center Grant R827453 and the U.S. Environmental Protection Agency (EPA) cooperative agreement No. R828060010. The authors thank Dirk Felton, NYSDEC, for his assistance in providing the ozone data. Special thanks go to Kenneth Demerjian, James Schwab, and others from SUNY Albany for being great hosts.
Address correspondence to Philip K. Hopke, Department of Chemical Engineering, Clarkson University, Potsdam, NY 13699-5708, USA. E-mail: hopkepk@clarkson.edu

such as the hypochlorite ion (OCl^-) and the superoxide anion (O_2^-) are collectively described as reactive oxygen species. In addition, there are organic peroxy radicals formed through the reaction of hydroxyl radicals or ozone with reactive hydrocarbon compounds. Atmospheric ROS is mainly generated from photochemical reactions in polluted air containing two main classes of precursor pollutants, volatile organic compounds (VOCs) and NO_x (Seinfeld and Pandis 1998). In the absence of sunlight, the mechanism of formation of ROS is highly influenced by the chemistry of the NO_3 radical (Wayne et al. 1991) and the OH radical formation from the reactions of ozone with alkenes (mainly biogenic VOCs) (Paulson and Orlando 1996).

Combustion of organic materials such as wood also can generate atmospheric ROS (Kao and Wang 2002). ROS appear in both the gas and particulate phase. Earlier studies looking at atmospheric ROS have focused mainly on ROS in the gas phase and in rainwater and cloud droplets (Sakugawa et al. 1993; Tsai et al. 1991). However, concentration data on ROS in the particulate phase is limited (Hung and Wang 2001; Hasson and Paulson 2003; Venkatachari et al. 2005). Hasson and Paulson (2003) suggested that most of the particle-bound ROS is H_2O_2, but observe greater ROS than would be present based on a Henry's Law model of uptake by the particles. However, they also observed much lower concentrations than Hung and Wang (2001) that they attributed to problems with the extraction procedure of the earlier work. In laboratory studies, Docherty et al. (2005) investigated the role of organic peroxides in secondary organic aerosol (SOA) formation from biogenic monoterpenes such as α-pinene and concluded that SOA was predominantly organic peroxides with the latter contributing anywhere between 47% and 85% of the total SOA mass. Ziemann (2002) postulated diacyl peroxides as a nucleating agent and major component of aerosol formed from reactions of ozone with cyclic alkenes such as cyclohexene and its homologues. Thus, the extent and nature of the ROS associated with particles is not yet well characterized.

Particles generated in diesel emissions, combustion aerosols from wood, incense, and so on are generally smaller than a few tenths of a micrometer in diameter. Particles in this size range have a rate of about 20–30%, of deposition in the alveolar regions of the respiratory tract (Hung and Wang 2001). Excessive ROS, either from exogenous or endogenous sources, exhibit a greater cytotoxic effect on cellular membrane integrity (Vallyathan et al. 1988), and consequently induce cell injury that may trigger a cascade of free radical reactions promoting disease processes. ROS has been implicated in the pathogenesis of many pulmonary diseases including asthma (Kehrer 1993), and has been known to play a role in the tumor promotional stage of carcinogenesis (Cerruti 1985). In contrast, most of the ROS in the gas phase have high solubility and molecular diffusivity, and are mostly absorbed by the mucus in the upper respiratory tract (Friedlander and Yeh 1998).

Ambient measurements of particulate ROS made in the winter of 2004, during the $PM_{2.5}$ Technology Assessment and Characterization Study—New York (PMTACS-NY) field campaign at Flushing, New York are presented. Previously, Venkatachari et al. (2005) examined the particle-bound ROS in the various size fractions of the ambient aerosols in Rubidoux, California and found that ROS concentrations correlated moderately with the intensity of photochemical reactions, smaller particles were observed to have higher ROS concentrations, and the general magnitude of ROS concentrations were found to be at least an order of magnitude higher than observed in Taipei (Hung and Wang 2001). This study examines the diurnal variation of ROS concentrations in the winter. It explores the relationship between ROS concentrations and ozone concentrations that were used as an indicator of the intensity of photochemical reactions. Secondary organic carbon (SOC) concentrations at the site are estimated by applying the EC tracer method (Turpin and Huntzicker 1995) on measured organic carbon (OC) and elemental carbon concentrations (EC). The effect of these carbonaceous components on the measured particulate ROS concentrations, as well as the statistical significance of their relationships with the ROS are examined. Furthermore, ROS concentrations are also compared with gas phase OH and HO_2 concentrations that were simultaneously measured at the site during this period. Finally, a comparison with results obtained in Rubidoux is presented.

EXPERIMENTAL SECTION

Sampling Location

During the period of January 12, 2004 to February 5, 2004, airborne particulate matter was sampled and analyzed for reactive oxygen species at the New York Supersite at Queens College. This site is located at 40° 43′ 42″ N, 73° 49′ 17″ W, about 14 kilometers west of Manhattan, and is close to both freeways and airports. The Long Island Expressway (495) and the Van Wyck Expressway (678) are both less than two kilometers from the site. Two international airports, John F. Kennedy and LaGuardia, are both within 12 kilometers of the sampling site. Prevailing wind direction in this region is predominantly northwesterly.

Instruments

Particle sampling was done using a Micro-Orifice Uniform Deposit Impactor® (MOUDI™, MSP, Minneapolis, USA) (Marple et al. 1991) and a Nano-MOUDI™ (MSP, Minneapolis, USA). The particles were collected on Nucleopore® polycarbonate filters (Whatman, 1 μm pore size, USA). The MOUDI™ is a rotating 10-stage cascade impactor with a sampling flow rate of 30 L/min. The Nano-MOUDI™ is a 3-stage cascade impactor, that is connected downstream of the MOUDI™ through a critical orifice in order to facilitate collection of nanometer sized particles. The flow rate through the Nano-MOUDI™ is 10 L/min. The cut sizes of the MOUDI™ are 18, 10, 5.6, 2.5, 1.8, 1, 0.56, 0.32, 0.18, 0.1, and 0.056 μm, whereas those of the Nano-MOUDI™ are 0.032, 0.018, and 0.010 μm.

Reagents

Rapid quantitative determination of ROS concentration can be performed with a fluorogenic probe such as dichlorofluorescin (DCFH). DCFH is a non-fluorescent reagent that becomes fluorescent dichlorofluorescin (DCF) upon reaction with ROS. DCFH was prepared from 2′, 7′-dichlorofluorescin diacetate (DCFH-DA) (Calbiochem, California, USA), according to the procedure provided by Cathcart et al. (1983). Mixing 0.5 mL of 1 mM DCFH-DA in ethanol with 2 mL of 0.01 N NaOH solution, yielded an unstable DCFH solution, which was incubated at room temperature in the dark for 30 minutes. The hydrolyzate was then neutralized with 10 mL sodium phosphate buffer solution to maintain a pH of 7.2 in the resulting solution. The solution was kept on ice without exposing it to the light until use. To catalyze the reaction between DCFH and the ROS, Immunopure® Horseradish peroxidase (HRP) (Pierce Chemical, Illinois, USA) was added to the DCFH solution in a ratio such that the working reagent of DCFH-HRP contained 2.2 units of HRP/mL of the reagent. DCFH has been proved to have a high sensitivity that is capable of detecting picomole levels of hydroperoxides (Cathcart et al. 1983). Scott et al. (1988) and Zhu et al. (1994) explored DCFH response to xanthine oxidase and iron/H_2O_2 exposures respectively under various conditions and suggested DCF formation from the superoxide, H_2O_2, and the OH radical oxidation as the reason for observed results. DCFH oxidized products induced by peroxyl radicals have also been documented (Adom and Liu 2005). Furthermore, it should also be noted that DCFH has been found to respond to peroxynitrite in biological assays (Kooy et al. 1997). Thus, its lack of specificity toward reactive oxygen species (LeBel et al. 1992), coupled with its positive response to all the oxidants constituting "ROS" have made it an appealing probe for studying toxicological phenomena, and has led to its wide use in biological systems for detecting oxidative activity and indicating oxidative stress. Recently, DCFH has also been used in the assay of particles for ROS formed from welding fumes (Antonini et al. 1998).

Procedure

Sampling was done at 3-hour intervals in the morning (8–11 A.M.), early afternoon (12–3 P.M.), late afternoon (4–7 P.M.), and at night (9 P.M.–12 A.M.) in order to determine the pattern of diurnal variation of ROS concentration. Field blanks were also collected. Subsequent to the particle collection, the sample filters and the field blanks were suspended in a 50 mL beaker containing 12.5 mL of 1 μM DCFH-HRP, and sonicated for 15 minutes to extract ROS from the particles, and then incubated at 37°C for a further 15 minutes. After incubation, each sample of the suspension was placed in clear 4-sided cuvettes (10 mm × 10 mm). Analysis of the samples for ROS was performed with the help of a Turner™ Quantech Digital Filter Fluorometer (model #FM109535). The cuvettes were inserted in the sample chamber of the Turner™ Fluorometer to measure the fluorogenic intensity of DCF in each sample and field blank. The measured fluorescent intensity of the field blanks (approximately 28–60% of the fluorescence of the particle samples) was subtracted from those of the particle samples to minimize the uncertainty arising from possible contamination during analysis. Background fluorescence caused due to autooxidation of DCFH or by the action of the added peroxidase is also taken care of in the analysis by subtracting the blank fluorescence from that of the sample. In order to correlate the fluorescent intensities and concentrations in terms of equivalent H_2O_2 concentrations (Hung and Wang 2001), an assay of standard solutions of H_2O_2 was performed. Solutions of 1.0, 2.0, 3.0, and 4.0×10^{-7} M H_2O_2 were prepared in 0.1 mL aliquots each and were added to 3 mL of the DCFH-HRP reagent mixture. Blanks were prepared with 0.1 mL distilled and deionized water instead of H_2O_2. Standard solutions and blanks were incubated at 37°C for 15 minutes, and the resulting fluorescent intensity was measured by the filter fluorometer. A calibration curve (shown in supplementary material, Figure S1) was drawn from the measured fluorescence of standard H_2O_2 solutions, and the fluorescence intensity data from the analysis of the samples was converted into equivalent H_2O_2 concentrations using the obtained calibration curve. In prior biological studies, it has been documented that removal of the diacetate groups in DCFH-DA may result in trace H_2O_2 production (Rota et al. 1999). However, we suggest that these are quantitatively insignificant sources of error, based on the observed background levels of DCF fluorescence. Myhre et al. (2003) came to the same conclusion based on results of tests they performed on cellular systems.

RESULTS AND DISCUSSION

ROS Concentrations

Sampling was performed in four 3-hour intervals through the course of a day to characterize particulate ROS concentrations and determine the diurnal variation in the concentration of ROS in the various size fractions of the Flushing aerosol. The results obtained are presented in Table 1. For the ambient aerosol in Flushing, the average total ROS concentrations expressed in terms of equivalent H_2O_2 concentrations were 1.149, 1.338, 1.176, and 1.056 nanomoles/m^3 during the sampling intervals between 8–11 A.M., 12–3 P.M., 4–7 P.M. and 9 P.M.–12 A.M., respectively. Smaller particles were observed to have higher ROS concentrations, especially particles in the 10–56 nm size range.

Lower concentrations of ROS were found in this study when compared to the study conducted in Rubidoux (Venkatachari et al. 2005). The lower concentrations can be attributed to any of the following: the study was conducted in winter when the temperatures and the intensity and duration of the solar flux was not conducive for photochemical reactions to produce free radicals. The presence of strong northwesterly winds for much of the period meant that not much reactive material was being brought to the area. With northwesterly flow, there are no major cities on the way to New York City. The high wind speeds lead

TABLE 1
ROS concentrations over the various size fractions of the Flushing aerosol, during the four sampling periods

	Equivalent H_2O_2 Concentrations in nanomoles/m^3											
	8–11 A.M.			12–3 P.M.			4–7 P.M.			9 P.M.–12 A.M.		
Size interval (μm)	Range	Mean	SD	Range	Mean	SD	Range	Mean	SD	Range	Mean	SD
>18	0.048–0.144	0.091	0.031	0.065–0.148	0.11	0.025	0.048–0.161	0.084	0.026	0.041–0.123	0.073	0.024
10–18	0.034–0.120	0.069	0.023	0.054–0.126	0.089	0.023	0.041–0.171	0.084	0.033	0.035–0.09	0.059	0.016
5.6–10	0.036–0.129	0.071	0.025	0.054–0.144	0.086	0.025	0.038–0.104	0.065	0.024	0.039–0.100	0.063	0.019
2.5–5.6	0.038–0.114	0.074	0.019	0.053–0.134	0.085	0.024	0.035–0.116	0.073	0.024	0.035–0.101	0.061	0.019
1.8–2.5	0.039–0.100	0.069	0.019	0.044–0.124	0.076	0.024	0.036–0.110	0.07	0.024	0.031–0.104	0.054	0.019
1.0–1.8	0.038–0.135	0.068	0.024	0.036–0.111	0.075	0.024	0.034–0.109	0.073	0.024	0.035–0.111	0.065	0.021
0.56–1.0	0.036–0.089	0.063	0.016	0.04–0.151	0.083	0.029	0.033–0.245	0.086	0.051	0.036–0.113	0.059	0.023
0.32–0.56	0.050–0.126	0.079	0.025	0.043–0.145	0.093	0.026	0.036–0.111	0.061	0.023	0.034–0.101	0.058	0.019
0.18–0.32	0.040–0.099	0.064	0.015	0.036–0.138	0.078	0.033	0.040–0.099	0.064	0.018	0.036–0.113	0.065	0.021
0.10–0.18	0.054–0.086	0.069	0.009	0.033–0.109	0.076	0.024	0.035–0.114	0.068	0.028	0.030–0.090	0.058	0.018
0.056–0.10	0.049–0.100	0.07	0.015	0.061–0.106	0.083	0.024	0.059–0.116	0.08	0.021	0.046–0.128	0.075	0.023
0.032–0.056	0.093–0.168	0.131	0.024	0.121–0.171	0.143	0.018	0.1–0.146	0.118	0.016	0.086–0.163	0.121	0.023
0.018–0.032	0.089–0.181	0.115	0.024	0.100–0.174	0.14	0.024	0.104–0.150	0.125	0.013	0.089–0.168	0.121	0.023
0.010–0.018	0.100–0.178	0.118	0.021	0.100–0.164	0.126	0.015	0.104–0.189	0.129	0.021	0.093–0.174	0.125	0.021
Sample Size	14			15			14			14		
Avg. Total ROS Conc.	1.149			1.338			1.176			1.056		
Std. Dev.	0.1099			0.1109			0.1528			0.1618		
Range	0.926–1.35			1.178–1.525			1.011–1.425			0.88–1.45		

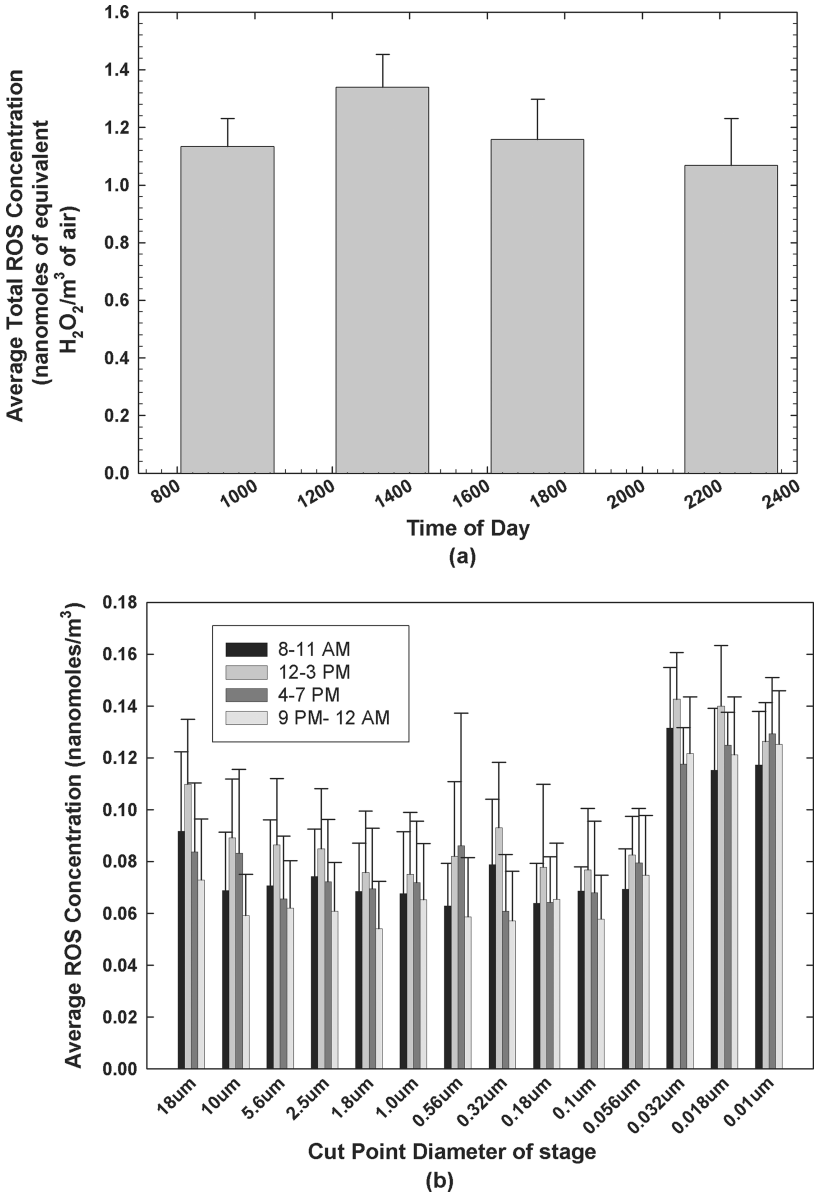

FIG. 1. Diurnal variations of (a) mean total particulate ROS concentrations and (b) mean stagewise ROS concentrations.

to high dilution and low residence time in source areas. Also, there were no smog episodes to provide the amount of precursors necessary for the production of a large amount of free radicals.

Figure 1a shows the diurnal variations in the average total ROS concentrations. The highest average total ROS concentrations occur during the midday sampling intervals. The nighttime ROS concentrations are comparable in magnitude being only slightly lower than the daytime levels. Although there is not a sharp drop in concentration during the evening, this diurnal pattern suggests that photochemical activity is the main source of the ROS. Primary emissions would be expected to come from motor vehicles operating on the nearby highways (Long Island and Van Wyck Expressways). However, they would show a peak concentration in the earliest time interval (8–11) when there would be the morning rush hour traffic coupled with the relatively lower mixing height that would persist from the overnight period. Given the peak activity in mid-afternoon, it appears that photochemistry is the main source of the observed oxidative activity.

The ozone levels were consistently low at night, with average concentrations of less than 10 ppbv, which suggests that the amount of fresh ROS being formed by the oxidation of alkenes by ozone is minimal. The nighttime levels seem to indicate the presence of some long-lived ROS species, mostly organic peroxides (Docherty et al. 2005) and thus potential for transport.

Figure 1b shows the trends in stagewise particle-bound ROS concentrations. There was no observable diurnal trend

in the stage-wise ROS concentrations. A two-level Analysis of Variance (ANOVA) of the size and time dependent ROS concentrations in the 10–56 nm stages with the corresponding concentrations in the other stages revealed that statistically significant higher ROS concentrations ($p < 0.001$) occurred in the Nano-MOUDI™ stages. This trend was observed in Rubidoux as well (Venkatachari et al. 2005). The disconnect in the concentrations of ROS in the Nano-MOUDI™ stages in Rubidoux were attributed to the condensation of vapor phase ROS onto the particles or the filters as a result of their adiabatic expansion at the low pressures encountered in the Nano-MOUDI™ stages. In Flushing, a disconnect in the ROS concentrations does occur in the Nano-MOUDI™ stages (see Figure S2a, supplementary material) although to a much lesser extent than was observed in Rubidoux. This result might be explained by the fact that the majority of the vapor-phase ROS was already condensed onto the particles at the lower winter temperatures of the order of –15°C to –10°C encountered throughout the period of the study. Hence, the concentration of particle-bound ROS in these stages might have been overestimated. It should be noted that this overestimation applies only to the ROS concentrations per stage for the Nano-MOUDI™ stages, and not the total ROS concentrations. The total Nano-MOUDI™ stage concentrations are found to be significantly different from, and lower than the total concentration of the MOUDI stages (see Figure S2b, supplementary material). Also, it should be noted that since 3-hour samples were collected, short-lived ROS having lifetimes substantially less than 3 hours cannot be estimated and hence the concentration of ROS might also be underestimated in this study. It is not possible to fully define the size distribution of the particle-bound ROS, but it is likely to be in the sub-micron range.

ROS-O_3 Correlation

Since photochemical reactions of chemical species accounts for a majority of the free radicals in the daytime atmosphere, the local intensity of photochemical reactions could be an important cause of the observed particle-bound ROS concentrations. Although O_3 can be transported, it is largely a result of local photodecomposition. In this study, the average ozone concentration was examined as a potential marker of the intensity of photochemical reactions as suggested by Hung and Wang (2001). The ozone data was obtained from standard photometric ozone monitors maintained by the New York State Department of Environmental Conservation (NYSDEC) at the site. The scatter plots of the average ozone concentrations and the corresponding ROS concentrations for the daytime sampling intervals are shown in Figure 2.

There is a weak correlation between the O_3 and the ROS concentrations that indicates the formation of ROS is promoted by enhanced photochemical activity. The correlation, as evidenced by the Pearson correlation coefficient, r, is highest for the 12–3 P.M. sampling interval since the local intensity of photochemical reactions would be maximum at this time. The lower correlation during the late afternoon sampling period of 4–7 P.M., might be due to the fact that the sampling was done during wintertime, when days were shorter and hence the local intensity of solar radiation would be low for most of this sampling period. In order to confirm that the relationship of ozone with ROS was significantly different, and that the regressions were statistically significant, a single factor ANOVA was performed (see supplementary material). The results of the ANOVA test indicated a significant difference ($p < 0.001$) and that the level of ozone affected the magnitude of the ROS concentrations. These results show that the local intensity of photochemical reaction was a moderate factor affecting the formation of particulate ROS in the daytime atmosphere. The absence of a more positive correlation maybe explained by the vertical mixing in the lower few kilometers, slow dry deposition to the surface, and local sources of NO such as motor vehicle traffic that destroys O_3. The particle-bound ROS include longer lived oxidative species that were formed multiple hours ago and transported to the site. Moreover, the chemistry of formation of the different constituents of ROS is complex. At this time, little is known about the specific constituents of the ROS and additional work is needed to elucidate their structure that would provide additional insights into their formation mechanisms. Their generation and binding to particles is affected by a variety of factors such as the concentrations of the precursor components, meteorological conditions such as solar radiation, water vapor concentration, temperature and pressure (Logan et al. 1981). For example, it has been observed that the yields of hydrogen peroxide increase from 1% in dry air to 9% in moist air, and the yields of other complex peroxides also increase substantially in the presence of water vapor (Reeves and Penkett 2003). It is apparent that ROS producing chemical systems are non-linear, and thus, the correlation with local O_3 concentrations can be expected to be relatively weak. This finding is consistent with previous studies (Hung and Wang 2001; Venkatachari et al. 2005).

ROS–SOC Correlation

Secondary organic carbon (SOC) refers to particulate material formed in the atmosphere through gas-to-particle conversion processes, most of which are photochemically driven. The ratio of the ambient concentrations of particulate OC to EC includes information about the extent of SOC formation, since primary OC and EC are mostly emitted by the same combustion source. Ambient ratios of OC/EC which are greater than this primary OC/EC ratio indicate secondary organic aerosol formation. Thus, secondary OC can be defined as:

$$OC_{sec} = OC_{tot} - OC_{pri}$$

and

$$OC_{pri} = EC \times (OC/EC)_{pri}$$

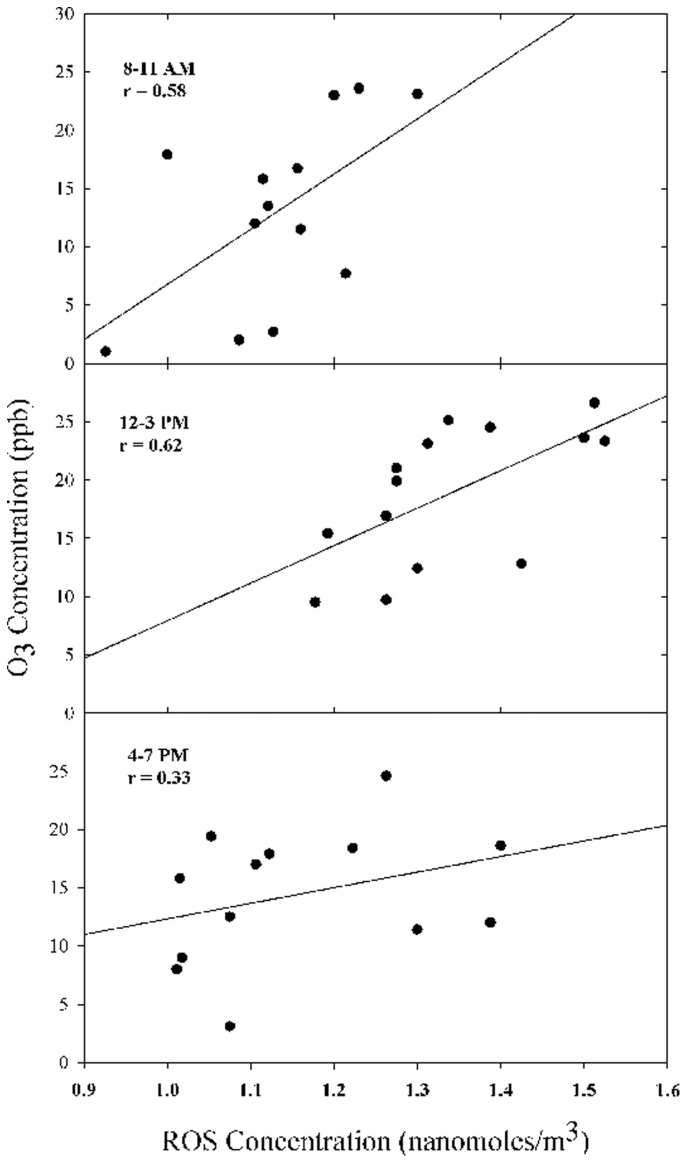

FIG. 2. Regression graphs showing correlation between mean ozone concentrations and mean total particulate ROS concentrations during the three daytime sampling periods.

where OC_{sec} is secondary OC, OC_{tot} is total OC, OC_{pri} is primary OC, and $(OC/EC)_{pri}$ is the primary ratio estimate. Further details on the method can be found elsewhere (Turpin and Huntzicker 1995). Based on the measured OC and EC, the upper bound of the primary OC/EC ratio was found to be 1.3 (Venkatachari et al. 2006), and was used to calculate SOC. Figure 3 shows the scatter plots of the estimated SOC concentrations and the corresponding particulate ROS concentrations for the sampling intervals. It is observed that the ROS is best correlated with SOC during the midday intervals, especially during the late afternoon. One-way ANOVA analyses were conducted between ROS and EC, OC, and estimated SOC, respectively (see supplementary material). A statistically significant relationship ($p < 0.05$) was observed only in the case of ROS and SOC. Thus, despite the lack of an observable strong correlation, the existence of a statistically significant correlation, as well as the consistency of the positive relationships between ROS and SOC for all the periods suggests that the measured ROS is photochemically driven. Scatter plots between ROS and EC and ROS and OC (Figures S3 and S4, supplementary material) were also constructed. Trends observed in this scatter plots, accompanied with the lack of a positive, statistically significant correlation ($p > 0.05$) from the ANOVA analyses conducted between them seem to indicate that primary emissions, especially from motor vehicles, are not a major source of the measured particle-bound ROS. However, it is not possible to ascertain their exact impact without

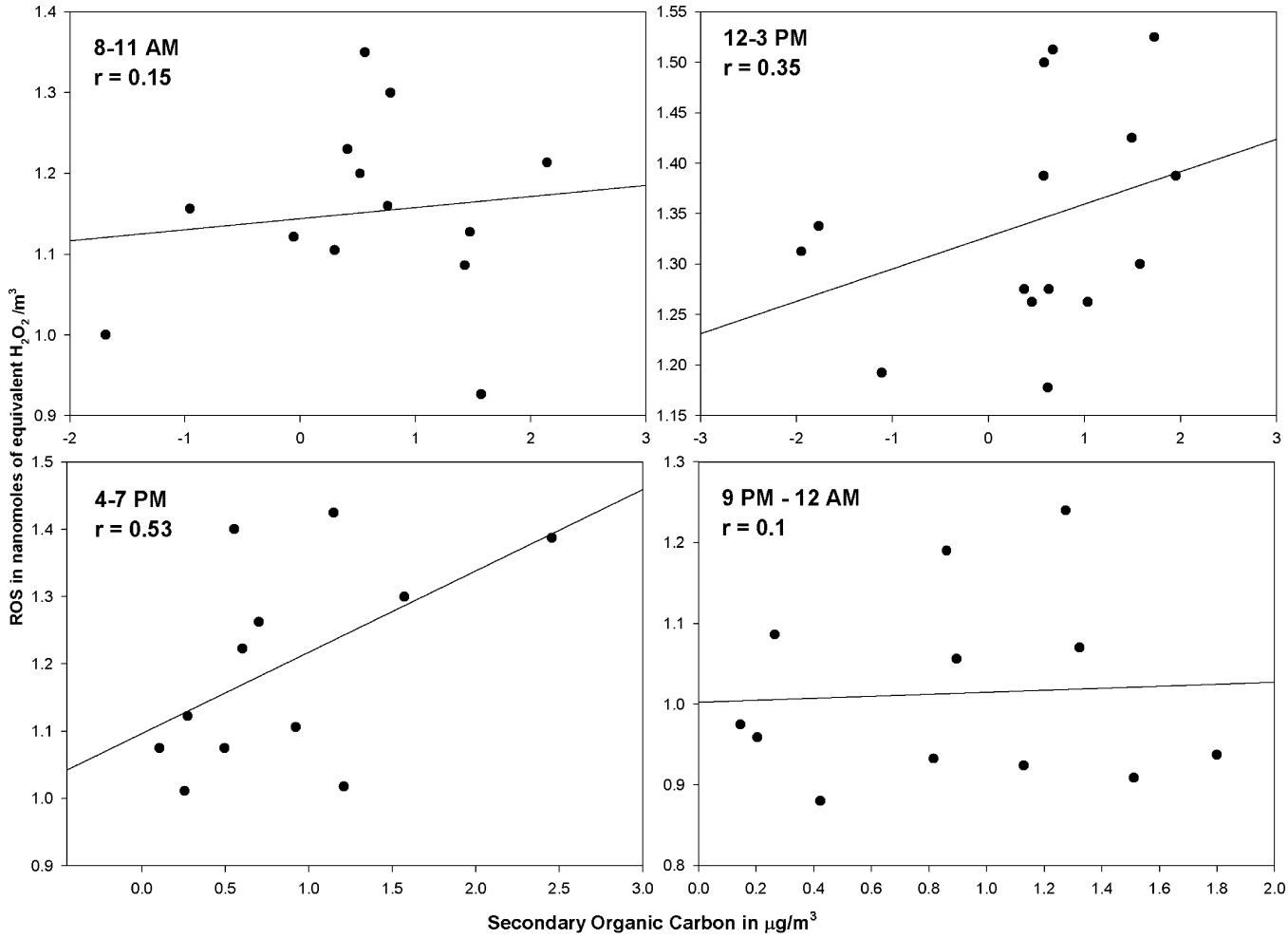

FIG. 3. Regression graphs showing correlation between estimated SOC concentrations and mean total particulate ROS concentrations during the sampling periods.

knowledge of the specific chemical nature of the observed ROS.

Correlation of ROS with Gas Phase OH and HO_2

Figure 4 shows the average concentration profiles of ROS and gas phase OH and HO_2 radicals over the period of sampling. The gas phase data was provided by the Penn State University group that did the measurements at the site during the study period. Laser Induced Fluorescence was used to measure gas phase OH and HO_2 radical concentrations. The results indicate the existence of, at best, a weak positive correlation. In order to confirm that the relationship of ROS with the gas phase radicals was significantly different, a single factor Analysis of Variance (ANOVA) was performed (see supplementary material). The results of the ANOVA test indicated that different levels of OH, HO_2, and OH+ HO_2 resulted in significantly different ($p < 0.001$) ROS concentrations. The weak correlation may represent the difference between relatively lower reactivity particle-bound ROS that accumulates over time and distance, and local photochemistry producing the gas phase radicals, since the OH and HO_2 radicals are not going to be transported over long distances. The lack of a more positive correlation of the particle-bound ROS, both with ozone as well as other gas phase oxidants, shows the decoupling of the particulate matter ROS from the gas phase oxidants. Also, a decreasing relationship between the ROS concentration and OH and HO_2 concentration was observed during the 9 P.M.–12 A.M. sampling period (graph not shown). One of the major reaction pathways for biogenic VOC's like isoprene and terpenes is their reaction with OH, removing it from the air and ultimately forming organic peroxyl radicals.

In an urban environment like New York City, CO, CH_4, and NMHC's also function as OH sinks leading to the formation of organic peroxides. A negative correlation might then be expected. Aerosol uptake of the species formed from the aforementioned pathways are expected to be the major contributors to the particle-bound ROS formed at night, since

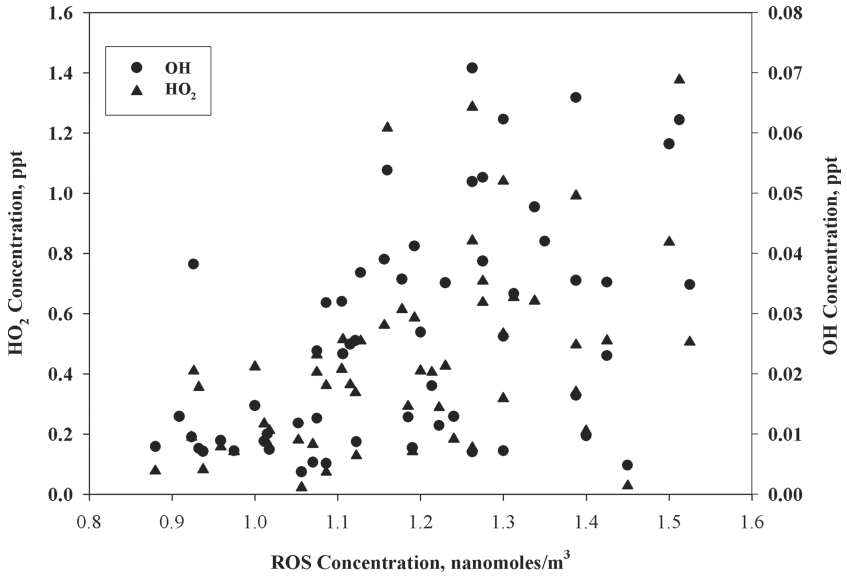

FIG. 4. Scatter plot of mean total particulate ROS with gas phase OH and HO_2 radical concentrations over the period of sampling.

at the low temperatures encountered during the study, nitrate radical chemistry would not play an important role in ROS formation.

CONCLUSIONS

Sampling of ambient aerosols was performed to characterize the particle-bound concentrations of ROS, their diurnal variation, and dependence on various factors. These measurements suggest that the local intensity of photochemical reactions, as indicated by the correlations found between the ROS and O_3 concentrations was a moderate factor in the formation of daytime ROS. The weak oxidative chemistry occurring during winter when this study was undertaken, coupled with the complex atmospheric chemistry of ROS, suggests that the weak correlation is to be expected. Observed correlations, or the lack thereof, of the measured ROS with EC, OC and estimated SOC concentrations at the site, further strengthen the argument for the photochemical nature of the measured ROS. The presence of comparable nighttime ROS during the sampling period might be indicative of the fact that the biogenic VOC-OH radical reaction pathway might be a dominant source of the nighttime ROS. Moderate correlations were found between the particle-bound ROS and gas phase HO_x concentrations. Further study is required to put these results in perspective with the ROS that is generated *in situ* in the tissues of the lung and to try and relate the exposure that people may receive of directly inhaled ROS to that which is generated *in situ*.

REFERENCES

Adom, K. K., and Liu, R. H. (2005). Rapid Peroxyl Radical Scavenging Capacity (PSSC) Assay for Assessing both Hydrophilic and Lipophilic Antioxidants, *J. Agric. Food Chem.* 53:6572–6580.

Antonini, J. M., Clarke, R. W., Krishnamurthy, G. G., Sreekanthan, P., Jenkins, N., Eagar, T. W., and Brian, J. D. (1998). Freshly Generated Stainless Steel Welding Fumes Induces Greater Lung Inflammation in Rats as Compared to Aged Fume, *Toxicol. Letters* 98:78–86.

Cathcart, R., Schwiers, E., and Ames, B. N. (1983). Detection of Picomole Levels of Hydroperoxides using a Fluorescent Dichlorofluorescein Assay, *Anal. Biochem.* 134:111–116.

Cerruti, P. A. (1985). Prooxidant States and Tumor Promotion, *Science* 227:375–381.

Docherty, K. S., Wu, W., Lim, Y. B., and Ziemann, P. J. (2005). Contributions of Organic Peroxides to Secondary Aerosol Formed from Reactions of Monoterpenes with O_3, *Environ. Sci. Technol.* 39:4049–4059.

Dockery, D. W., Schwartz, J., and Spengler, J. D. (1992). Air Pollution and Daily Mortality: Associations with Particulate and Acid Aerosols, *Environ. Res.* 59:362–373.

Friedlander, S. K, and Yeh, E. K. (1998). The Submicron Atmospheric Aerosol as a Carrier of Reactive Chemical Species: Case of Peroxides, *Appl. Occ. Environ. Hyg.* 13(6):416–420.

Hasson, A. S., and Paulson, S. E. (2003). An Investigation of the Relationship Between Gas-Pase and Aerosol-Borne Hydroperoxides in Urban Air. *J. Aerosol Sci.*, 34:459–468.

Hung, H.-F., and Wang, C.-S. (2001). Experimental Determination of Reactive Oxygen Species in Taipei Aerosols, *J. Aerosol Sci.* 32:1201–1211.

Kao, M.-C., and Wang, C.-S. (2002). Reactive Oxygen Species in Incense Smoke, *Aerosol Air Qual. Res.* 2:61–69.

Kehrer, J. P. (1993). Free Radicals as Mediators of Tissue Injury and Disease, *Crit. Rev. Toxicol.* 23:21–48.

Kooy, N. W., Royall, J. A., and Ischiropoulos, H. (1997). Oxidation of 2′, 7′–Dichlorofluorescein by Peroxynitrite, *Free Radic. Res.* 27:245–254.

LeBel, C. P., Ischiropoulos, H., and Bondy, S. C. (1992). Evaluation of the Probe 2′, 7′-Dichlorofluorescin as an Indicator of Reactive Oxygen Species Formation and Oidative Stress, *Chem. Res. Toxicol.* 5:227–231.

Logan, J. A., Prather, M. J., Wofsy, S. C., and Elroy, M. B. (1981). Tropospheric Chemistry: A Global Perspective, *J. Geophys. Res.* 86:7210–7254.

Marple, A. V., Rubow, L. K., and Behm, M. S. (1991). A Micro-Orifice uniform Deposit Impactor (MOUDI)—Description, Calibration and Use, *Aerosol Sci. Tech.* 14:434–446.

Mauderly, J. L. (1998). Toxicology of Diesel Engine Emissions. In Health Effects of Particulate Matter in Ambient Air (J. Vostal, ed.), *Air and Waste Manage. Assoc.* 573–580.

Myhre, O., Andersen, J. M., Aarnes, H., and Fonnum, F. (2003). Evaluation of the probe 2′, 7′-Dichlorofluorescein Diacetate, Luminol, and Lucigenin as Indicators of Reactive Species Formation, *Biochem. Pharm.* 65:1575–1582.

Paulson, S. E., and Orlando, J. J. (1996). The Reactions of Ozone with Alkenes: An Important Source of HO_x in the Boundary Layer, *Geophys. Res. Letters* 23:3727–3730.

Reeves, C. E., and Penkett, S. A. (2003). Measurements of Peroxides and What they Tell Us, *Chem. Rev.* 103:5199–5218.

Rota C., Fann Y. C., and Mason R. P. (1999). Phenoxyl free Radical Formation during the Oxidation of the Fluorescent dye 2′, 7′-Dichlorofluorescein by Horseradish Peroxidase. Possible Consequences for Oxidative Stress Measurements, *J. Biol. Chem.* 274:28161–28168.

Sakugawa, H., Kaplan, I. R., and Shepard, L. S., 1993. Measurement of H_2O_2, Aldehydes and Organic Acids in Los Angeles Rainwater: Their Sources and Deposition Rates, *Atmospheric Environment* 27B(2), 203–219.

Seinfeld, J. H., and Pandis, S. N. (1998). *Atmospheric Chemistry and Physics: From Air Pollution to Climate Change*. Wiley Publishers, New York.

Scott, J. A., Homcy, C. J., Khaw, B. A., and Rabito, C. A. (1988). Quantitation of Intracellular Oxidation in a Renal Epithelial Cell Line, *Free Rad. Bio. Med.* 4:79–83.

Stohs, S. J., and Bagchi, D. (1995). Oxidative Mechanisms in the Toxicity of Metal Ions, *Free Rad. Bio. Med.* 18(2):321–336.

Tsai, W., Cohen, Y., Sakugawa, H., and Kaplan, I. R. (1991). Hydrogen Peroxide and Ozone Levels in Los Angeles: A Screening Level Evaluation, *Atmos. Environ.* 25:67–78.

Turpin, B. J., and Huntzicker, J. J., (1995). Identification of Secondary Organic Aerosol Episodes and Quantitation of Primary and Secondary Organic Aerosol Concentrations during SCAQS, *Atmos. Environ.* 29:3527–3544.

Vallyathan, V., Shi, X., Dalal, N. S., Irr, W., and Castranova, V. (1988). Generation of free Radicals from Freshly Fractured Silica Dust: Potential Role in Acute Silica–Induced Lung Injury, *Amer. Rev. Resp. Diseases* 138:1213–1219.

Venkatachari, P., Hopke, P. K., Grover, B. D., and Eatough, D. J., (2005). Measurement of Particle–Bound Reactive Oxygen Species in Rubidoux Aerosols, *J. Atmos. Chem.* 50:49–58.

Venkatachari, P., Zhou, L., Hopke, P. K., Schwab, J. J., Demerjian, K. L., Weimer, S., Hogrefe, O., Felton, D., and Rattigan, O. (2006). An Intercomparison of Measurement Methods for Carbonaceous Aerosol in the Ambient Air in New York City, *Aerosol Sci. Tech.* 40:788–795.

Wayne, R. P., Barnes, I., Biggs, P., Burrows, J. P., Canosa–Mas, C. E., Hjorth, J., LeBras, G., Moortgat, G. K., Perner, D., Poulet, G., Restelli, G., and Sidebottom, H. (1991). The Nitrate Radical: Physics, Chemistry and the Atmosphere, *Atmos. Environ.* 25A:1–203.

Zhu, H., Bannenberg, G. L., Moldeus, P., and Shertzer, H. G. (1994). Oxidation Pathways for the Intracellular Probe 2′,7′- Dichlorofluorescein, *Arch. Toxicol.* 68:582–587.

Ziemann, P. J. (2002). Evidence for Low-Volatility Diacyl Peroxides as a Nucleating Agent and Major Component of Aerosol Formed from Reactions of Ozone with Cyclohexene and Homologous Compounds, *J. Phys. Chem. A* 106:4390–4402.

SUPPLEMENTARY MATERIAL

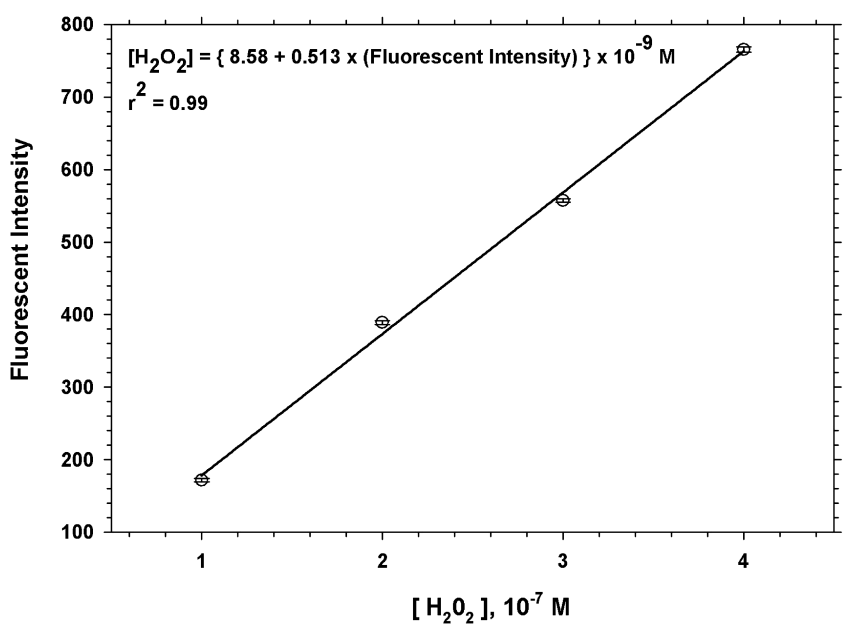

Figure S1: Calibration curve of the measured fluorescence of standard H_2O_2 solutions, where M is the molarity of the solution.

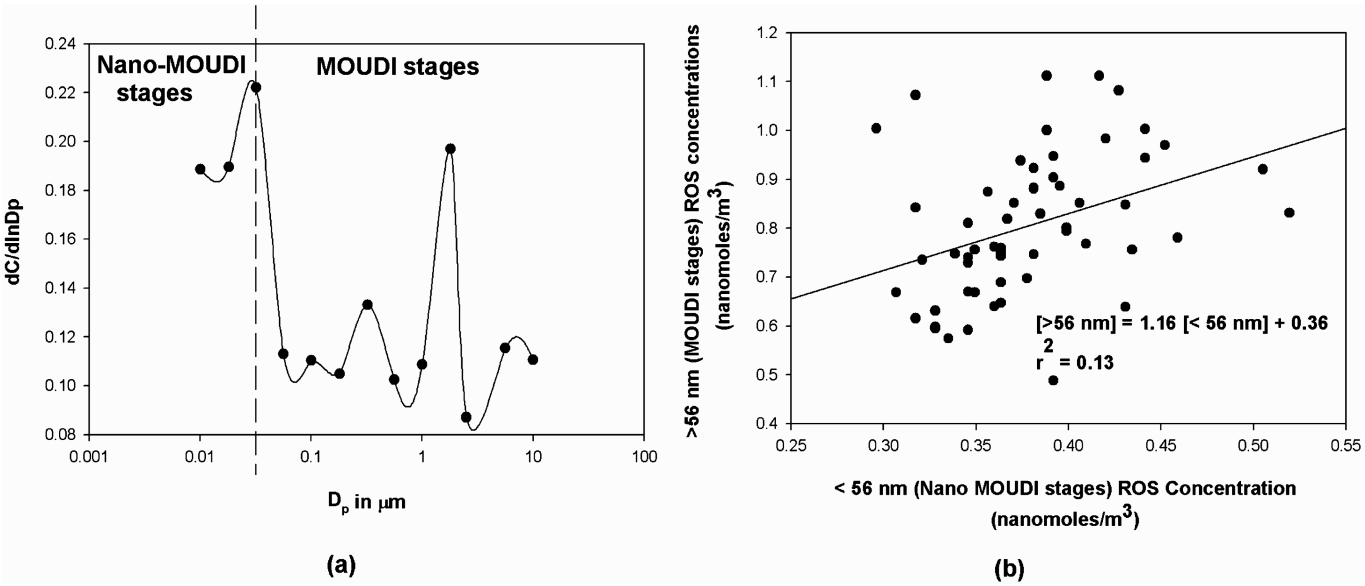

Figure S2: (**a**) Stagewise concentration distribution curve, and (**b**) scatter plot of the total ROS concentration in the Nano-MOUDI stages versus the total ROS concentration in the MOUDI stages.

SECTION S1: ROS-OZONE CORRELATION: ANOVA TEST RESULTS

ROS Conc. in nanomoles/m^3	Ozone in ppb
0.926	1
1.086	2
1.128	2.7
1.08	3.1
1.214	7.7
1.011	8
1.018	9
1.178	9.5
1.263	9.7
1.3	11.4
1.16	11.5
1.105	12
1.388	12
1.3	12.4
1.075	12.5
1.425	12.8
1.121	13.5
1.193	15.4
1.115	15.8
1.015	15.8
1.156	16.7
1.263	16.9
1.106	17
1	17.9
1.123	17.9
1.223	18.4
1.4	18.6
1.053	19.4
1.275	19.9
1.275	21
1.2	23
1.3	23.1
1.313	23.1
1.525	23.3
1.23	23.6
1.5	23.6
1.388	24.5
1.263	24.6
1.338	25.1
1 513	26.6

Ozone in ppb			
A: 0–10	B: 10–15	C: 15–20	D: 20–30
0.926	1.3	1.193	1.275
1.086	1.16	1.115	1.2
1.128	1.105	1.015	1.3
1.075	1.388	1.156	1.313
1.214	1.3	1.263	1.525
1.011	1.075	1.106	1.23
1.018	1.425	1	1.5
1.178	1.121	1.123	1.388
1.263		1.223	1.263
		1.4	1.338
		1.053	1.513
		1.275	

Single factor ANOVA			
Source of variance	F ratio	P value	Critical F ratio ($\alpha = 0.05$)
Between groups	8.46	0.000219	2.866

The Analysis of Variance (ANOVA) test is a statistical test for the heterogeneity of means by the analysis of group variances. Here, ANOVA is used to test for the presence of a statistically significant difference in ROS concentrations with ozone concentrations. Towards this end, the ROS concentrations are classified into four groups based on the corresponding ozone concentrations of 0–10, 10–15, 15–20, and 20–30 ppb. A statistically significant distribution is said to be obtained if the P value (defined as the probability that a variate would assume a value greater than or equal to the observed value strictly by chance) is less than the significance level, denoted by α. Also, the F ratio, which is the ratio of two independent estimates of the variance of a normal distribution, should be greater than a certain critical value calculated based on the significance level (α) and the number of degrees of freedom. As observed in the tables above, these criteria are satisfied, and hence, the ROS concentrations are affected significantly differently by different ozone concentrations.

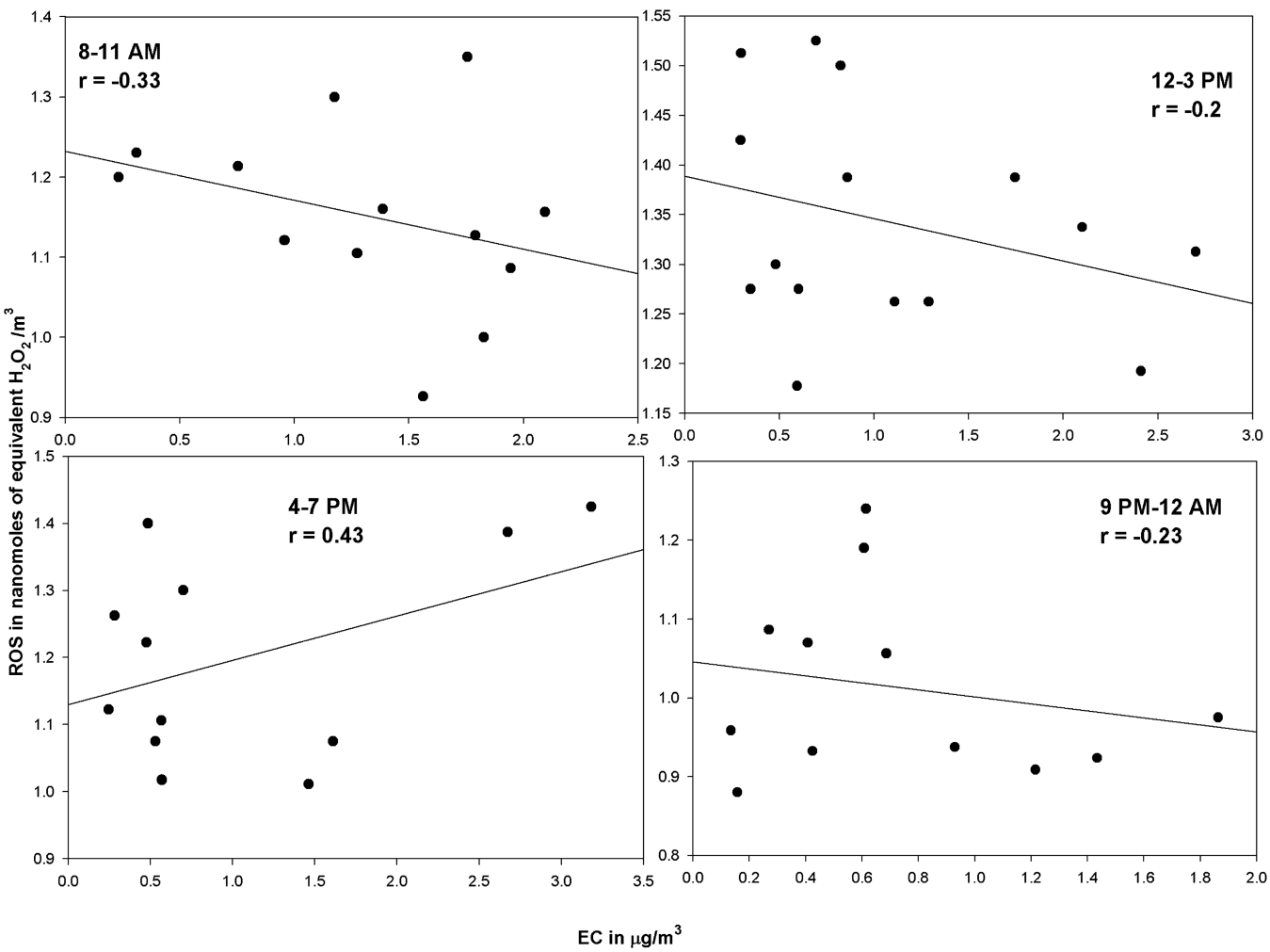

Figure S3: Regression graphs showing correlation between measured EC concentrations and mean total particulate ROS concentrations during the sampling periods.

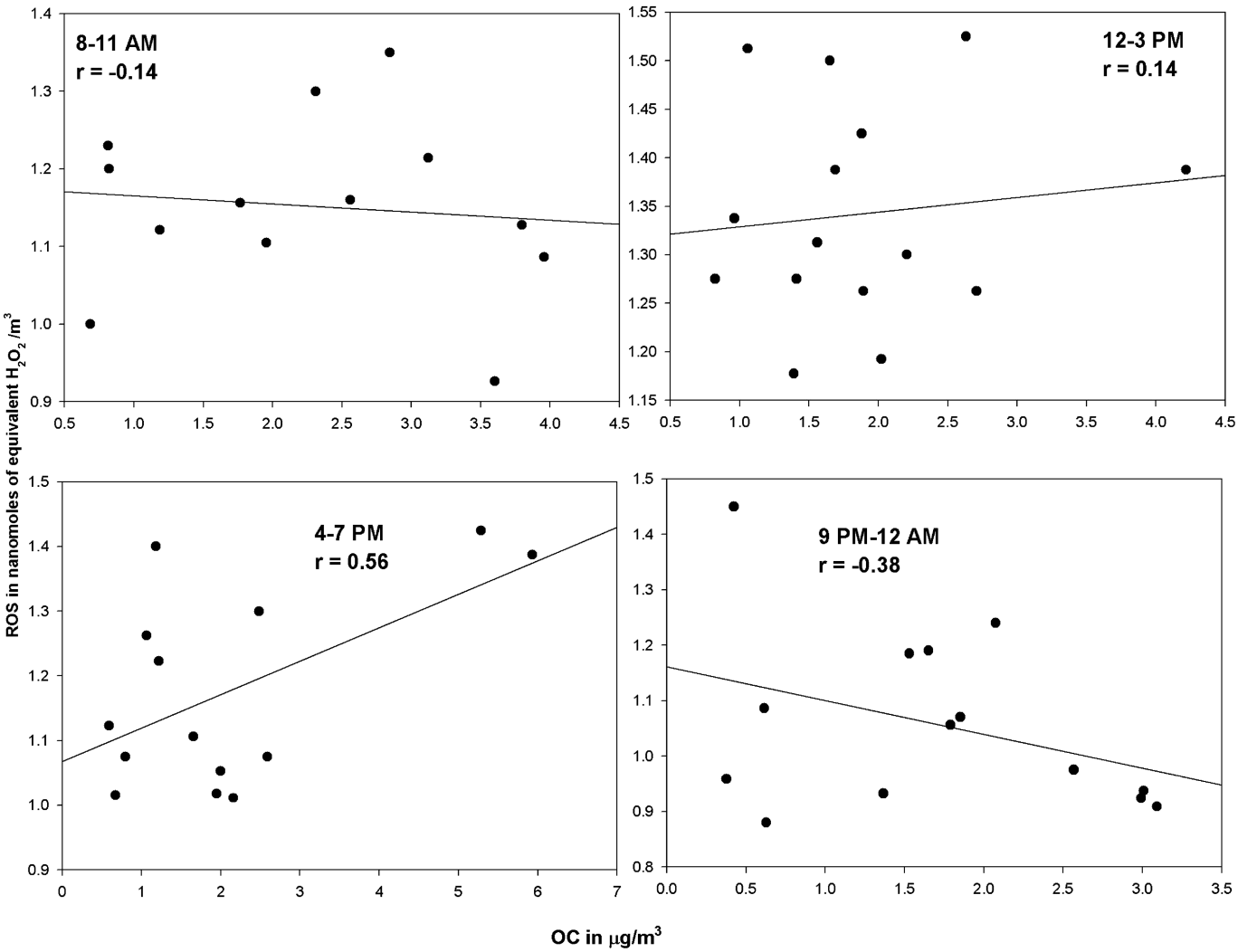

Figure S4: Regression graphs showing correlation between measured OC concentrations and mean total particulate ROS concentrations during the sampling periods.

SECTION S4: CORRELATION OF ROS WITH SOC, EC AND OC: ANOVA TEST RESULTS

S4-1: ROS-SOC ANOVA

SOC Conc. in μg/m^3		
A: < 0.55	B: 0.55–1.1	C:>1.1
1.313	1.400	1.425
1.338	1.350	1.018
1.000	1.388	1.086
1.193	1.500	1.128
1.156	1.223	1.425
1.121	1.178	0.926
1.075	1.275	1.300
1.011	1.513	1.300

SOC Conc. in μg/m^3		
A: <0.55	B: 0.55–1.1	C:>1.1
1.123	1.263	1.525
1.105	1.160	1.388
1.275	1.300	1.214
1.230	1.106	1.388
1.263	1.263	
1.075		
1.200		

Single factor ANOVA

Source of variance	F-ratio	P value	Critical F-ratio ($\alpha = 0.05$)
Between groups	3.54	0.039	3.25

S4-2: ROS-EC ANOVA

EC Conc. in μg/m^3			
A: <0.45	B: 0.45–0.70	C: 0.7–1.5	D: >1.5
0.959	1.223	1.214	0.926
0.880	1.300	1.500	1.075
1.200	1.400	1.388	1.388
1.123	1.075	0.938	1.350
1.086	1.106	1.121	1.128
1.263	1.018	1.263	1.000
1.425	1.178	1.300	0.975
1.513	1.275	0.909	1.086
1.230	1.190	1.105	1.156
1.275	1.240	1.263	1.338
1.070	1.056	1.160	1.193
0.933	1.525	0.924	1.388
	1.300	1.011	1.313
			1 475

Single factor ANOVA

Source of variance	F-ratio	P value	Critical F-ratio ($\alpha = 0.05$)
Between groups	0.36	0.78	2.79

S4-3: ROS-OC ANOVA

OC Conc. in μg/m^3			
A: <1.1	B: 1.1–1.8	C: 1.8–2.6	D: >2.6
0.959	1.400	1.070	1.525
1.450	1.121	1.425	1.263
1.123	1.223	1.263	1.350
1.086	0.933	1.018	0.924
0.880	1.178	1.105	0.938
1.015	1.275	1.053	0.909
1.000	1.185	1.193	1.214
1.075	1.313	1.240	0.926
1.230	1.500	1.011	1.128
1.200	1.190	1.300	1.086
1.275	1.106	1.300	1.388
1.338	1.388	1.300	1.425
1.513	1.156	1.160	1.388
1.263	1.056	0.975	
		1.075	

Single factor ANOVA

Source of variance	F-ratio	P value	Critical F-ratio ($\alpha = 0.05$)
Between groups	0.24	0.86	2.78

In order to explore the effect of primary emissions on the observed ROS concentrations, linear regressions were carried out between the measured ROS concentrations and EC and OC concentrations observed at the site. Additionally ANOVA analyses were carried out to investigate the statistical significance of the effect of the EC and OC concentrations on the observed particle-bound ROS concentrations. It was observed, as seen in Figures S3 and S4, that both EC and OC, in general, exhibit poor, negative correlations with the observed ROS concentrations. Furthermore, the ANOVA analyses between these components seem to indicate no statistical relevance of primary EC and OC concentrations on the ROS concentrations. The observed positive correlations during the afternoon periods between, the EC and OC and ROS concentrations, when there is maximum photochemical activity, again serves to reinforce our hypothesis of the photochemical activity driving the ROS concentrations. Additionally, as seen above, the ANOVA analysis when carried out between the observed SOC concentrations, and the ROS concentrations indicates the presence of a statistically relevant relationship between the two (P-value > α; F-ratio > Critical F-ratio).

SECTION S3: CORRELATION OF ROS WITH GAS PHASE OH AND HO_2: ANOVA TEST RESULTS

S3-1: ROS-OH ANOVA

OH Conc. in ppt			
A: 0–0.0095	B: 0.0095–0.025	C: 0.025–0.04	D: 0.04–0.08
1.056	1.4	1.121	1.193
1.45	1.015	1.3	1.35
1.086	1.223	1.2	1.338
1.07	1.053	1.086	1.263
1.263	1.075	1.105	1.275
0.938	1.185	1.313	1.16
1.3	0.909	1.525	1.5
0.975	1.24	1.23	1.513
1.018	1	1.425	1.3
0.933	1.388	1.388	1.388
1.19	1.214	1.178	1.263
0.88	1.425	1.128	
1.123	1.106	0.926	
1.011	1.075	1.275	
0.959	1.115	1.156	
0.924			

Single factor ANOVA

Source of variance	F-ratio	P value	Critical F-ratio ($\alpha = 0.05$)
Between groups	6.661	0.00067	2.779

S3-2: ROS-HO_2, ANOVA

HO_2 Conc. in ppt		
A: <0.25	B: 0.25–0.5	C: >0.5
1.056	1.223	1.525
1.45	1.185	1.128
1.086	1.3	1.425
0.88	1.121	1.106
0.938	1.388	1.3
1.123	0.933	1.156
1.19	1.086	1.193
0.975	1.115	1.178
1.263	1.214	1.275
0.959	1.075	1.338
1.07	0.926	1.313
1.015	1.2	1.275
1.053	1.105	1.5
1.24	1	1.263
0.924	1.23	1.388
1.4	1.075	1.3
1.018	1.388	1.16
1.011		1.263
		1.513

Single factor ANOVA

Source of variance	F-ratio	P value	Critical F-ratio ($\alpha = 0.05$)
Between groups	10.036	0.000211	3.179

S3-3: ROS-($OH + HO_2$) ANOVA

($OH + HO_2$) Conc. in ppt		
A: <0.3	B: 0.3–0.5	C: >0.5
1.056	1.185	1.388
1.45	1.3	1.106
1.086	1.388	1.525
0.88	1.121	1.425
0.938	0.933	1.128
1.123	1.115	1.3
0.975	1.086	1.156
1.19	1.075	1.193
1.263	1.214	1.178
0.959	1.2	1.275
1.07	1	1.313
1.015	1.105	1.338
1.053	0.926	1.275
1.24	1.23	1.263
0.924	1.075	1.5
1.018		1.388
1.4		1.3
1.011		1.16
1.223		1.263
		1.513

Single factor ANOVA

Source of variance	F-ratio	P value	Critical F-ratio ($\alpha = 0.05$)
Between groups	10.036	0.000211	3.179

ANOVA analyses were conducted on ROS, OH and HO_2 concentrations to provide the statistical strength to the arguments made in the main text. As observed above, there appears to be a significant relationship between the gas phase radicals and the measured ROS concentrations. In all three cases, the criteria for statistical significance, as alluded to before, are satisfied. Thus, there is statistically different ROS for different OH, HO_2 and $OH + HO_2$ concentrations.